Research Square

Preprints are preliminary reports that have not undergone peer review.
They should not be considered conclusive, used to inform clinical practice,
or referenced by the media as validated information.

Hamiltonian dynamics from pure dissipation

Daniel Stilck França

dsfranca13@gmail.com

University of Copenhagen https://orcid.org/0000-0001-9699-5994

Zhong-Xia Shang

University of Hong Kong

Article

Keywords:

Posted Date: July 31st, 2026

DOI: https://doi.org/10.21203/rs.3.rs-10130455/v1

License: This work is licensed under a Creative Commons Attribution 4.0 International License.
Read Full License

Additional Declarations: There is **NO** Competing Interest.

Hamiltonian dynamics from pure dissipation

Zhong-Xia Shang[1, *] and Daniel Stilck França[1, †]

[1] *Department of Mathematical Sciences, University of Copenhagen, Universitetsparken 5, 2100 Denmark*

The fundamental difference between closed and open quantum dynamics lies in their environmental interaction: closed systems are perfectly isolated and evolve reversibly under unitary Hamiltonian dynamics, whereas open systems continuously couple to an external bath, resulting in irreversible dissipation and information loss. In this work, we show internal Hamiltonian dynamics can be "faked" via external pure dissipation, i.e., Lindbladians without a coherent Hamiltonian part. More concretely, we show that, in a GKSL representation with zero explicit Hamiltonian, bounded-norm dissipative generators can approximate Hamiltonian dynamics within ϵ error in diamond norm using $\mathcal{O}(t^2/\epsilon)$ evolution time. We further prove that for time-independent dynamics this $\mathcal{O}(t^2/\epsilon)$ scaling is in the worst case, necessary and optimal from a geometric perspective, which captures the fundamental decoherence cost for catching up with the speed of Hamiltonian dynamics. For practical considerations, we establish an autonomous QDRIFT protocol and show how to exponentially improve the dependence on ϵ for expectation value estimation via extrapolations. Our construction leads to various implications, including the BQP-completeness of purely dissipative dynamics even before reaching approximate equilibrium, a Zeno-adjacent state-independent freezing effect, the no super-quadratic fast-forwarding theorem of a class of purely dissipative dynamics, and reducing Lindbladian simulation cost via gauge changing.

Introduction.—The dynamics of any physical systems are governed by a combination of internal interactions and external coupling to an environment. For a quantum system described by a d-dimensional Hilbert space $\mathcal{H} \cong \mathbb{C}^d$, the most general trace-preserving and completely positive Markovian evolution is described by the Gorini–Kossakowski–Sudarshan–Lindblad master equation (Lindbladian) [1, 2]

$$\frac{d\rho}{dt} = -i[H, \rho] + \sum_i \left(F_i \rho F_i^\dagger - \frac{1}{2}\{\rho, F_i^\dagger F_i\} \right). \tag{1}$$

Here, the first term captures the internal, coherent evolution driven by the system Hamiltonian $H \in \mathbb{C}^{d\times d}$, while the second term captures the external interactions mediated by the jump operators $\{F_i\} \subset \mathbb{C}^{d\times d}$. When external interactions are completely absent, the system is closed; it evolves unitarily and reversibly, preserving all quantum information. Conversely, the inclusion of the jump operators defines an open quantum system, where continuous interaction with a bath drives irreversible dissipation and decoherence [3].

Understanding how to simulate quantum systems and the effect of dissipation or decoherence is a central theoretical pursuit in quantum mechanics, with profound practical implications for quantum information and quantum computing. Especially, a recent wave of dissipation-based quantum algorithms has emerged, spanning Gibbs state [4–6] and ground state [7–9] preparation, solving differential equations [10], and optimization [11]. The performance, advantages, and inherent limitations of these dissipative approaches, especially when compared to traditional coherent algorithms [12], are deeply rooted in how open and closed dynamics interface and diverge [6].

To interrogate this boundary, we ask: *can coherent Hamiltonian dynamics be approximately reproduced by purely dissipative interactions, and if so, at what cost?* While Stinespring dilation [13] allows open systems to be modeled via closed dynamics, it does so by artificially expanding the Hilbert space to encompass the entire bath, thereby redefining the system-environment partition and converting external interactions into internal ones. However, if we restrict our view to the system alone, the fundamentally distinct physical origins and time-reversal properties of these two mechanisms suggest they cannot substitute for one another. Even though the gauge invariance [3] of the Lindbladian allows a certain level of freedom of interconversions, finding F_i such that

$$\sum_i \left(F_i \rho F_i^\dagger - \frac{1}{2}\{\rho, F_i^\dagger F_i\} \right) = -i[H, \rho] \tag{2}$$

holds exactly is impossible for any nonzero H [14].

In this work, we demonstrate that the internal, coherent Hamiltonian interactions can be well mimicked by strictly external, dissipative ones. Specifically, we prove that purely dissipative Lindbladians (i.e. Lindbladians with only

* zhongxia.shang@math.ku.dk
† dsfranca@math.ku.dk

$\{F_i\}$ and no H in eq. (1)) can achieve approximate ideal t-time Hamiltonian evolution within an error ϵ in diamond norm using an evolution time of $\mathcal{O}(t^2/\epsilon)$. This scaling shows that this imitation is not only possible but also efficient with no exponential overheads in time, system size or precision. Since the purely dissipative dynamics is fundamentally irreversible, we further show that this $\mathcal{O}(t^2/\epsilon)$ Lindbladian evolution time is actually necessary and optimal to simulate the reversible Hamiltonian dynamics in the worst case. We prove this via geometry: how to maximize the rotational speed (Hamiltonian dynamics) while minimizing the radial one (decoherence). Later, we show an autonomous QDRIFT [15] protocol and an extrapolation-based expectation value estimation method as practical applications. We also give several implications of our results for various topics, including the complexity class of dissipative dynamics, Zeno effect, fast-forwarding dissipative dynamics, and Lindbladian simulations.

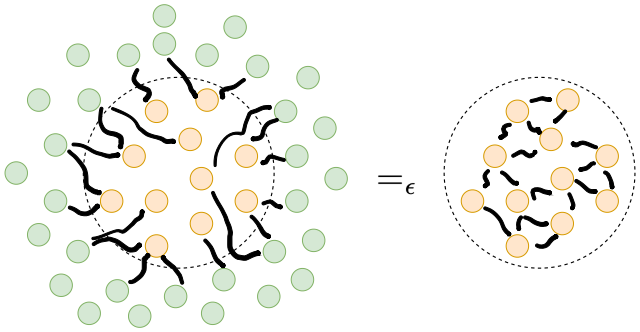


FIG. 1. The physical meaning of theorem 1. Our construction essentially says that for any closed quantum system characterized by the Hamiltonian H with zero external dissipation, we can always find a purely dissipative open quantum system with zero internal Hamiltonian to efficiently mimic its dynamics.

Hamiltonian dynamics via dissipation.— Our construction is simple and direct. Consider a purely dissipative, single-jump Lindbladian

$$\frac{d\rho}{dt} = \mathcal{L}[\rho] = F\rho F^\dagger - \frac{1}{2}\{F^\dagger F, \rho\}, \tag{3}$$

i.e. in GKSL form with only one jump (albeit not necessarily traceless). If we set $F = I - i\delta H$, then we will have

$$\frac{d\rho}{dt} = -i\delta[H, \rho] + \delta^2\left(H\rho H - \frac{1}{2}\{H^2, \rho\}\right), \tag{4}$$

where the first term is a δ-strength Hamiltonian dynamics and the second term is δ^2-strength dissipation when viewing H as a jump operator, which has recently been found to have deep connections with quantum phase estimation [16]. Based on eq. (4), we obtain the following theorem.

Theorem 1. *By setting $\delta = \epsilon/t$, the purely dissipative, single-jump Lindbladian eq. (3) can approximate the Hamiltonian dynamics $e^{\mathcal{L}_H t}[\rho] = e^{-iHt}\rho e^{iHt}$ within ϵ error in diamond distance [17] in the sense that $\sup_{0\le s\le t}\left\|e^{\mathcal{L}\frac{T}{t}s} - e^{\mathcal{L}_H s}\right\|_\diamond \le \epsilon$, by an evolution time*

$$T = \mathcal{O}\left(\|H\|_\infty^2 t^2 \epsilon^{-1}\right). \tag{5}$$

We give detailed proofs in App. A, which uses Duhamel's Identity [18] to bound the distance between dynamics via the distance between the Liouvillian operators. The theorem 1 is surprising in terms of the physical picture as shown in fig. 1. Closed quantum systems have zero dissipation and non-zero internal Hamiltonians, while purely dissipative open quantum systems have zero internal Hamiltonians but non-zero dissipation. Therefore, these two types of systems are exactly the opposite of each other and should have fundamentally different dynamics. However, our result here shows that in fact the purely dissipative one can efficiently mimic the other with only an overhead that matches the first-order product formula-based Hamiltonian simulation method [19].

The design of the jump operator is not unique, and we show two generalizations. First, as long as $F = I - \delta A + \mathcal{O}(\delta^2)$ and the anti-Hermitian part of A is H, then the Lindbladian evolution time to achieve the same goal in theorem 1 requires

$$T = \mathcal{O}\left(\|A\|_\infty^2 t^2 \epsilon^{-1}\right). \tag{6}$$

A direct example of such a jump is $F = e^{-iH\delta}$, which is unitary short-time Hamiltonian dynamics itself.

Second, one may argue $F = I - i\delta H$ is not physical since H is a global operator, whereas physical jumps should be local. But note that we can actually localize jumps by increasing their number. Suppose H has the decomposition $H = \sum_i H_i$, with H_i local, then for each term, we can assign a jump operator $F_i = I - i\delta H_i$, and the resulting multi-jump purely dissipative Lindbladian can approximate the Hamiltonian dynamics by an evolution time

$$T = \mathcal{O}\left(\sum_i \|H_i\|_\infty^2 t^2 \epsilon^{-1}\right). \tag{7}$$

This version is especially relevant for platforms with local dissipative control [20], and it shows that coherent many-body dynamics can be generated from local open-system primitives with only polynomial overhead. We later generalize this idea to our autonomous QDRIFT

One may notice that in all the above constructions, the jumps have the form $I + \delta O + \mathcal{O}(\delta^2)$ with O some operator. In fact, we can prove this is the only possible form for smooth, purely dissipative Lindbladians that mimic the Hamiltonian dynamics.

Proposition 1 (Uniqueness up to $O(\delta^2)$)**.** *Let $\{\mathcal{L}_{D,\delta}\}_{0\le\delta<\delta_0}$ be a smooth family of purely dissipative Lindbladians on a finite-dimensional system, and let*

$$\mathcal{L}_H(\rho) := -i[H, \rho]. \tag{8}$$

Assume that there exists $t_0 > 0$ such that

$$\varepsilon(\delta) := \sup_{0\le s\le t_0} \left\| e^{\frac{s}{\delta}\mathcal{L}_{D,\delta}} - e^{s\mathcal{L}_H} \right\|_\diamond \xrightarrow[\delta\to 0]{} 0. \tag{9}$$

Then

$$\mathcal{L}_{D,\delta} = \delta\mathcal{L}_H + O(\delta^2) \tag{10}$$

in diamond norm.

We refer to App. C for the detailed proof. But note that our proof boils down to showing that Eq. (9) implies constraints on how the family of smooth Lindbladians $\mathcal{L}_{D,\delta}$ must behave at different orders of δ. An interesting remark here is that while shifting the Hamiltonian (adding identity) is trivial and only introduces a global phase, shifting the jump operator can fundamentally change the dynamics.

We finish this section by introducing a corollary of theorem 1. Since Hamiltonian dynamics can be recast as dissipation, therefore, we can actually convert any Lindbladian into a pure dissipation form. For the general form eq. (1), we can construct a purely dissipative Lindbladian with jump operators F' where we let $F'_0 = I - i\delta H$ and let $F'_i = \sqrt{\delta} F_i$, then by setting $\delta = \epsilon/t$, to simulate the original Lindbladian for an evolution time t within error ϵ, the required new Lindbladian evolution time is

$$T = \mathcal{O}\left(\|H\|_\infty^2 t^2 \epsilon^{-1}\right). \tag{11}$$

Geometric Lower Bound.— Now, we want to show that since the dissipation is irreversible and fundamentally different from the Hamiltonian dynamics after all, the $\mathcal{O}(t^2/\epsilon)$ cost is what you have to pay in the worst case, as illustrated in the theorem below:

Theorem 2. *There exist families of Hamiltonians $H \in \mathbb{C}^{2\times 2}$ such that if a purely dissipative Lindbladian of the form*

$$\mathcal{L}_D(\rho) = \sum_{j=1}^m \left(F_j \rho F_j^\dagger - \tfrac{1}{2}\{F_j^\dagger F_j, \rho\}\right), \quad \|F_j\|_\infty \le C, \tag{12}$$

can simulate the target Hamiltonian dynamics for an evolution time t within an diamond-distance error ϵ uniformly in time

$$\sup_{0\le s\le t} \left\| e^{\mathcal{L}_D \frac{T}{t} s} - e^{\mathcal{L}_H s} \right\|_\diamond \le \epsilon, \tag{13}$$

then the total Lindbladian evolution time T must satisfy the lower bound

$$T = \Omega\left(\frac{\|H\|_\infty^2}{mC^2} t^2 \epsilon^{-1}\right). \tag{14}$$

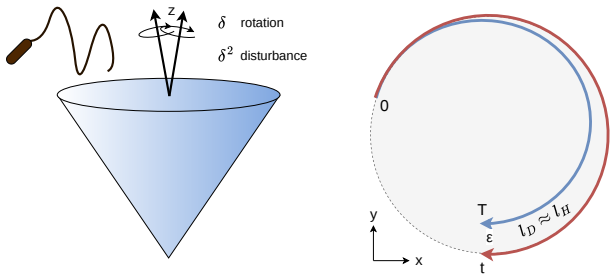


FIG. 2. **Left:** Hamiltonian dynamics via dissipation can be compared to driving a top via a whip. Since we want to rotate the top (Hamiltonian dynamics) via an external whip (environment), the rotation of a δ-strength is inevitably accompanied by radial disturbance (dissipation) of δ^2-strength. **Right:** Under the uniform-in-time error restriction eq. (13), the dissipative trajectory (blue) should be close to the Hamiltonian trajectory (red). As results, the radial distance between the ideal state and the Lindbladian evolved state should be within ϵ, and the trajectory length of the dissipative dynamics (l_D) should be close to the trajectory length of the Hamiltonian dynamics (l_H).

We have two remarks for theorem 2. First, the mC^2 factor in eq. (14) matches the block encoding cost in the digital Lindbladian simulation algorithms on quantum computers [21–29]. Second, the reason we ask the uniform-in-time error assumption is to avoid the adversarial cheating where the Lindbladian doesn't actually simulate the Hamiltonian dynamics but only approximates the unitary map $e^{\mathcal{L}_H t}$ at the specific time t.

The proof idea of theorem 2 is from a geometric point of view. Since the lower bound cares about the worst case, we can analyze the lower bound via a single-qubit system where we consider approximating $H = \nu\sigma_z/2$ via eq. (12). By mapping the qubit's density matrix to a Bloch vector $r \in \mathbb{R}^3$, the purely dissipative Lindbladian eq. (12) can be recast as an affine Bloch equation of the form $\dot{r} = Br + c$ [13] with

$$B = S + [\boldsymbol{\omega}\times]. \tag{15}$$

The matrix $[\boldsymbol{\omega}\times]$ (representing cross product by $\boldsymbol{\omega}$) is real and antisymmetric, representing the effective rotational speed that attempts to mimic the target Hamiltonian dynamics. The matrix S is real, symmetric, and strictly negative semi-definite ($S \preceq 0$). This component drives the inevitable radial contraction, pulling the state away from the boundary of the Bloch sphere and representing irreversible decoherence.

Since both $[\boldsymbol{\omega}\times]$ and S emerge from eq. (12), we prove that they have the relation

$$|\boldsymbol{\omega}|^2 \leq mC^2(-\mathrm{Tr}S). \tag{16}$$

This indicates that one cannot increasing the rotational speed without increasing the radial decoherence. The $|\boldsymbol{\omega}|^2$ versus $-\mathrm{Tr}S$ have been seen in eq. (4) with the δ-strength Hamiltonian part and the δ^2-strength dissipative part. We can also understand this from fig. 2 left, where we can imagine the Hamiltonian dynamics via dissipation as rotating a top via a whip. Since the internal Hamiltonian is zero, top cannot rotate by itself, and can only rely on the external force of whip, therefore, it is impossible to rotate the top without radial disturbance.

Under the uniform-in-time requirement eq. (13), we want the dissipative trajectory on the Bloch sphere to be close to the Hamiltonian trajectory as shown in fig. 2 right. This leads to two further consequences. First, S should be small such that the decoherence won't make the radial distance between the Bloch surface and the Lindbladian evolved state from a pure initial state to go beyond ϵ. We prove S must satisfy

$$-\mathrm{Tr}(S) \leq \frac{6\epsilon}{T}. \tag{17}$$

Second, $|T\boldsymbol{\omega}|$ should be large such that the length of the dissipative trajectory l_D can catch the length of the Hamiltonian trajectory $l_H = \nu t$, which relates to the so-called quantum speed limit [30–32]. We prove that $|\boldsymbol{\omega}|$ must satisfy

$$|\boldsymbol{\omega}| \geq \frac{\nu t}{8T}. \tag{18}$$

By combining eq. (16), eq. (17), and eq. (18), we proof theorem 2. Detailed proofs can be found in App. B.

Autonomous QDRIFT and extrapolation.— Our construction also gives a measurement-native realization of QDRIFT [15]. The details of the construction are discussed in App. D and we only give an overview here. Consider

a Pauli Hamiltonian

$$H = \sum_{\ell=1}^{L} h_\ell P_\ell, \qquad P_\ell = P_\ell^\dagger, \qquad P_\ell^2 = I, \tag{19}$$

and suppose that the Pauli products P_ℓ are available as dissipative readout or loss channels. Instead of implementing the coherent Pauli rotations used in standard QDRIFT, we introduce displaced Pauli jump operators

$$F_{\ell,\delta} = \sqrt{\gamma_\ell}\, I - i\delta \frac{h_\ell}{\sqrt{\gamma_\ell}} P_\ell, \qquad \gamma_\ell > 0. \tag{20}$$

Since $F_{\ell,\delta}^\dagger F_{\ell,\delta} = (\gamma_\ell + \delta^2 h_\ell^2/\gamma_\ell) I$, the click statistics are state-independent: the bath supplies the randomness, but no outcome-conditioned feedback is required. The corresponding purely dissipative generator satisfies

$$\sum_\ell \mathcal{D}_{F_{\ell,\delta}} = \delta \mathcal{L}_H + \delta^2 \sum_\ell \frac{h_\ell^2}{\gamma_\ell} \mathcal{Z}_{P_\ell}, \qquad \mathcal{Z}_P[\rho] = P\rho P - \rho. \tag{21}$$

Thus, after the same time rescaling as in theorem 1, the leading term is the target Hamiltonian evolution, while the subleading term is precisely the sampling-induced Pauli dephasing. If the total available displaced-channel strength is fixed as $\Gamma = \sum_\ell \gamma_\ell$ and $\lambda = \sum_\ell |h_\ell|$, the optimal allocation is

$$\gamma_\ell^\star = \Gamma \frac{|h_\ell|}{\lambda}. \tag{22}$$

For this choice, the jump labels are sampled with probabilities $p_\ell = |h_\ell|/\lambda$, exactly as in QDRIFT, and the rescaled generator takes the Poissonized QDRIFT form

$$\frac{1}{\delta} \sum_\ell \mathcal{D}_{F_{\ell,\delta}} = \mathcal{L}_H + \frac{\delta\lambda}{\Gamma} \sum_\ell |h_\ell| \mathcal{Z}_{P_\ell}. \tag{23}$$

Consequently,

$$\sup_{0\le s\le t} \left\| e^{(s/\delta)\sum_\ell \mathcal{D}_{F_{\ell,\delta}}} - e^{s\mathcal{L}_H} \right\|_\diamond \le \frac{2t\delta\lambda^2}{\Gamma}. \tag{24}$$

Choosing $\delta = \Theta(\epsilon\Gamma/(t\lambda^2))$ gives a dissipative evolution time

$$T = \frac{t}{\delta} = O\left(\frac{t^2\lambda^2}{\Gamma\epsilon}\right), \tag{25}$$

with an expected number of autonomous jumps $O(t^2\lambda^2/\epsilon)$, matching the usual QDRIFT scaling.

The difference is operational: the random Pauli rotations are generated by continuously running dissipative channels rather than by a classical randomized circuit scheduler. This makes the construction especially natural in architectures where high-weight Pauli measurements are native but coherent high-weight Pauli rotations are expensive.

Finally, for observable estimation rather than channel simulation, one can vary δ and classically Richardson-extrapolate the measured expectation values to the $\delta \to 0$ limit, in the spirit of qFLO [33]. More quantitatively, for the rescaled dissipative flow

$$e^{(t/\delta)\mathcal{L}_\delta} = e^{t(\mathcal{L}_H + \delta\mathcal{R})}, \tag{26}$$

the parameter δ plays the role of a controllable step size, and expectation values are analytic in δ. An m-point Richardson extrapolator cancels the first $m-1$ powers of this artificial dissipative bias, giving an intrinsic extrapolation error of order

$$O\left[\|b\|_1 \left(\frac{et\|\mathcal{R}\|_\diamond \delta_{\max}}{m}\right)^m\right], \tag{27}$$

where $\|b\|_1$ is the ℓ_1 norm of the extrapolation weights. Using the well-conditioned qFLO nodes [33], one has $\|b\|_1 = O(\log m)$, so choosing $m = \Theta(\log(1/\epsilon))$ reduces the largest required dissipative evolution time to

$$T_{\max} = O\big(t^2\|\mathcal{R}\|_\diamond \log(1/\epsilon)\big), \tag{28}$$

instead of the physical-channel scaling $O(t^2\|\mathcal{R}\|_\diamond/\epsilon)$. For autonomous QDRIFT with the optimal allocation, $\|\mathcal{R}\|_\diamond \leq 2\lambda^2/\Gamma$, hence

$$T_{\max} = O\left(\frac{t^2\lambda^2}{\Gamma}\log(1/\epsilon)\right), \mathbb{E}N_{\max} = O\left(t^2\lambda^2\log(1/\epsilon)\right). \tag{29}$$

This improvement applies to observable estimation via signed classical post-processing, not to implementing a single CPTP channel, and therefore does not contradict the lower bound in theorem 2.

Implications.—We now show several direct implications of our results.

1. Purely dissipative dynamics is BQP-complete.—A direct implication of our result is that purely dissipative dynamics is BQP-complete [34] beyond the fixed point. Since Hamiltonian dynamics is BQP-complete, theorem 1 indicates the purely dissipative Lindbladian is BQP-hard, which combining with the fact that Lindbladian can be efficiently simulated by repeated short-time unitary transformations plus tracing out operations via Stinespring dilation [13, 21, 23], leads to the BQP-complete result. An important remark here is that, previously, the BQP-complete results [6, 35, 36] of dissipation are all about the fixed point where the universal quantum computation is embedded into the steady states of the dissipative Lindbladian. Our result is different from the existing ones on BQP completeness of Lindbladians in the literature [6, 35, 36] in the sense that we do not encode the computation into properties of a (quasi)stationary state of the dynamics. Other results [37] achieve universality of Lindbladian dynamics by introducing auxiliary 'timer gadgets' to orchestrate sequential measurement-based operations. However, this typically requires significant spatial overhead in the form of complex lattice geometries and auxiliary clock qubits, overheads which are not present in our simple construction.

2. A novel Zeno-adjacent freezing mechanism. Quantum Zeno effect [38] states that strong and frequent measurements (or jump operators with large norms in the language of Lindbladian) can sometimes freeze the system's evolution. The mechanism of the traditional Zeno effect is to construct strong dissipators $\mathcal{L}_D[\rho] = \sum_i \left(F_i\rho F_i^\dagger - \frac{1}{2}\{\rho, F_i^\dagger F_i\}\right)$, which is so strong, such that the system can ignore the internal Hamiltonian and is forced to stay in the steady subspace where $\mathcal{L}_D[\rho] = 0$, also known as the Zeno subspace [39]. Our theorem 1 also leads to a fundamentally different mechanism of quantum Zeno effect. Suppose the system Hamiltonian is H, and we know H, then to freeze the dynamics, we can simply introduce a jump operator $F = \delta^{-1/2}(I + i\delta H)$. Then we have

$$\frac{d\rho}{dt} = -i[H,\rho] + F\rho F^\dagger - \frac{1}{2}\{\rho, F^\dagger F\} = \mathcal{O}(\delta). \tag{30}$$

Thus, setting $\delta = \epsilon/t$ can make sure $\|\rho(0) - \rho(t)\|_1 = \mathcal{O}(\epsilon)$. The idea of this new mechanism is to actively generate the reversal time evolution via dissipation to cancel out the system evolution. While both require large dissipation, the biggest difference between these two mechanisms is that the traditional mechanism can only freeze states that are inside the Zeno subspace, while ours can freeze any state.

3. No super-quadratic fast forwarding for a class of Lindbladians.—A central result in Hamiltonian simulation is the no fast-forwarding theorem [40, 41], which states that there exist no universal (meaning for any H) Hamiltonian simulation algorithms that can simulate t-time Hamiltonian dynamics within a constant precision $\epsilon = 1/4$ using sublinear costs in t. For the class of purely dissipative Lindbladian we considered ($F = I - i\delta H$), we can simply let H be the sparse parity check Hamiltonian [40, 42] used in the Hamiltonian no-fast-forwarding proof and set $\delta = \epsilon/t = 1/4T$, then we have $T = \mathcal{O}(t^2)$. If this Lindbladian can be super-quadratically fast-forwarded, i.e. $o(\sqrt{T})$, we will conflict with the query lower bound of the parity check problem, implying this class of Lindbladians cannot be fast-forwarded beyond quadratic. On the other hand, this also indicates that this class of Lindbladians has the possibility to be quadratically fast-forwarded in some cases, which, if true, will be another class of fast-forwardable Lindbladians beyond the recent progress [16, 43, 44]. We want to emphasize that we cannot simply use the t-time Hamiltonian dynamics to simulate the T-time Lindbladian evolution and claim achieving the quadratic fast-forwarding since the δ^2-strength of the dissipation is fixed and prevents the simulation error to be arbitrarily small. This raises the question of how to construct fast-forwarding algorithms for these Lindbladians.

4. Reducing Lindbladian simulation cost via gauge changing.—One way to understand theorem 1 is via the gauge freedom of Lindbladians. For H and F_i in eq. (1), we can do a gauge transform [3] while keeping the Liouvillian operator and therefore, the dynamics unchanged

$$\text{Jump: } F_i \to F_i' = \sum_j U_{ij}F_j + c_i I, \tag{31}$$

$$\text{Hamiltonian: } H \to H' = -\frac{i}{2}\sum_i \left(c_i^* F_i' - c_i F_i'^\dagger\right), \tag{32}$$

where U is unitary, c_i are arbitrary complex numbers. If we let $H = 0$ and $F_i = I - i\delta H$, then by setting $U = I$ and $c_i = -1$ we will have $H' = \delta H$ and $F' = -i\delta H$, which recovers eq. (4). In the context of simulating Lindbladian on quantum computers, given the Hamiltonian H and jump operators F_i, the algorithmic cost is then proportional to $\|H\|_\infty + \sum_i \|F_i\|_\infty^2$ [21–29]. For the Lindbladian we considered in theorem 1, we have $\|F\|_\infty = \mathcal{O}(1)$ while $\|H'\|_\infty + \sum_i \|F'\|_\infty^2 = \mathcal{O}(\delta)$. Therefore, while the gauge transform of the Lindbladian doesn't change the actual dynamics, it indeed can drastically change the simulation cost. This suggests that, if we want to simulate a Lindbladian on a quantum computer, instead of directly putting the Hamiltonian and jumps into the simulation algorithms, we can first find a better gauge with smaller norms and simulating the Lindbladian in that gauge will result in a lower cost.

Discussions.—In this work, we show the Hamiltonian dynamics can be efficiently simulated via pure dissipation via explicit construction (theorem 1) and prove it matches the $\Omega(t^2/\epsilon)$ lower bound (theorem 2). It is worth contrasting our result with a line of work on emergent unitary dynamics from dissipation initiated by [45, 46] and extended by [47]. These works consider a strongly dissipative Lindbladian $\mathcal{L}_0$ admitting a non-trivial manifold of steady states, perturbed by a weak Hamiltonian term λH. In the limit $\lambda \to 0$ with time rescaled as $\tau = \lambda t$, the effective dynamics projected onto the steady-state manifold becomes unitary, generated by a projected Hamiltonian PHP. The setup we consider here is fundamentally different in three respects. First, our Lindbladian has no Hamiltonian term at all: the coherent dynamics is generated entirely by the dissipator. Second, our construction does not rely on the existence of a non-trivial steady-state manifold: the target unitary evolution is approximated on the entire Hilbert space, not on a projected subspace. Third, we provide a quantitative error bound with matching upper and lower bounds of order t^2/ϵ, whereas the dissipation-projected dynamics literature is primarily concerned with the qualitative emergence of unitarity and its geometric structure. Our $\Omega(t^2/\epsilon)$ lower bound is also naturally dual to the $\mathcal{O}(t^2/\epsilon)$ overhead identified by [23] for the reverse direction of simulating Lindblad evolution via Hamiltonian evolution on a dilated system, with a similar scaling appearing in the repeated-interactions simulation of [28].

Several directions can be further explored. For example, whether and when it is possible and how to achieve the quadratic fast-forwarding for our considered Lindbladians as explained in Implication 3. Also, while in Implication 4, we explain the importance of choosing gauge in Lindbladian simulations, accurately estimating $\|H\|_\infty + \sum_i \|F_i\|_\infty^2$ is actually QMA-hard [48]. This raises the question of how to find a better gauge in a practical way.

ACKNOWLEDGMENTS

Z.S. would like to thank Weijie Xiong and Wenjun Yu for insightful discussions. D.S.F. and Z.S. thank Aram Harrow for interesting discussions. D.S.F. acknowledges financial support from the Novo Nordisk Foundation (Grant No. NNF20OC0059939 Quantum for Life). D.S.F. and Z.S. acknowledge support by the ERC grant GIFNEQ 101163938.

[1] V. Gorini, A. Kossakowski, and E. C. G. Sudarshan, Completely positive dynamical semigroups of n-level systems, Journal of Mathematical Physics **17**, 821 (1976).
[2] G. Lindblad, On the generators of quantum dynamical semigroups, Communications in mathematical physics **48**, 119 (1976).
[3] H.-P. Breuer and F. Petruccione, *The theory of open quantum systems* (OUP Oxford, 2002).
[4] C.-F. Chen, M. Kastoryano, F. G. Brandão, and A. Gilyén, Efficient quantum thermal simulation, Nature **646**, 561 (2025).
[5] C. Rouzé, D. Stilck França, and Á. M. Alhambra, Optimal quantum algorithm for gibbs state preparation, Physical Review Letters **136**, 060601 (2026).
[6] C.-F. Chen, H.-Y. Huang, J. Preskill, and L. Zhou, Local minima in quantum systems, in *Proceedings of the 56th Annual ACM Symposium on Theory of Computing* (2024) pp. 1323–1330.
[7] T. S. Cubitt, Dissipative ground state preparation and the dissipative quantum eigensolver, arXiv preprint arXiv:2303.11962 (2023).
[8] Z. Ding, C.-F. Chen, and L. Lin, Single-ancilla ground state preparation via lindbladians, Physical Review Research **6**, 033147 (2024).
[9] Y. Zhan, Z. Ding, J. Huhn, J. Gray, J. Preskill, G. K.-L. Chan, and L. Lin, Rapid quantum ground state preparation via dissipative dynamics, Physical Review X **16**, 011004 (2026).
[10] Z.-X. Shang, N. Guo, D. An, and Q. Zhao, Designing a nearly optimal quantum algorithm for linear differential equations via lindbladians, Physical Review Letters **135**, 120604 (2025).
[11] Z. Chen, Y. Lu, H. Wang, Y. Liu, and T. Li, Quantum langevin dynamics for optimization, Communications in Mathematical Physics **406**, 52 (2025).

[12] A. M. Dalzell, S. McArdle, M. Berta, P. Bienias, C.-F. Chen, A. Gilyén, C. T. Hann, M. J. Kastoryano, E. T. Khabiboulline, A. Kubica, *et al.*, Quantum algorithms: A survey of applications and end-to-end complexities, arXiv preprint arXiv:2310.03011 (2023).

[13] M. A. Nielsen and I. L. Chuang, *Quantum computation and quantum information* (Cambridge university press, 2010).

[14] P. Hayden and J. Sorce, A canonical hamiltonian for open quantum systems, Journal of Physics A: Mathematical and Theoretical **55**, 225302 (2022).

[15] E. Campbell, Random compiler for fast hamiltonian simulation, Physical review letters **123**, 070503 (2019).

[16] Z.-X. Shang, N. Guo, P. Rebentrost, A. Aspuru-Guzik, T. Li, and Q. Zhao, Fast-forwardable lindbladians imply quantum phase estimation, arXiv preprint arXiv:2510.06759 (2025).

[17] A. Y. Kitaev, A. Shen, and M. N. Vyalyi, *Classical and quantum computation*, 47 (American Mathematical Soc., 2002).

[18] L. C. Evans, *Partial differential equations*, Vol. 19 (American mathematical society, 2022).

[19] S. Lloyd, Universal quantum simulators, Science **273**, 1073 (1996).

[20] P. M. Harrington, E. J. Mueller, and K. W. Murch, Engineered dissipation for quantum information science, Nature Reviews Physics **4**, 660 (2022).

[21] M. Kliesch, T. Barthel, C. Gogolin, M. Kastoryano, and J. Eisert, Dissipative quantum church-turing theorem, Physical review letters **107**, 120501 (2011).

[22] A. M. Childs and T. Li, Efficient simulation of sparse markovian quantum dynamics, arXiv preprint arXiv:1611.05543 (2016).

[23] R. Cleve and C. Wang, Efficient quantum algorithms for simulating lindblad evolution, arXiv preprint arXiv:1612.09512 (2016).

[24] X. Li and C. Wang, Simulating markovian open quantum systems using higher-order series expansion, arXiv preprint arXiv:2212.02051 (2022).

[25] W. Yu, X. Li, Q. Zhao, and X. Yuan, Lindbladian simulation with logarithmic precision scaling via two ancillas, Physical Review Letters **135**, 160602 (2025).

[26] S. Peng, X. Sun, Q. Zhao, and H. Zhou, Quantum-trajectory-inspired lindbladian simulation (2024), arXiv preprint arXiv:2408.10505.

[27] Z. Ding, X. Li, and L. Lin, Simulating open quantum systems using hamiltonian simulations, PRX quantum **5**, 020332 (2024).

[28] M. Pocrnic, D. Segal, and N. Wiebe, Quantum simulation of lindbladian dynamics via repeated interactions, Journal of Physics A: Mathematical and Theoretical **58**, 305302 (2025).

[29] J. Kato, K. Wada, K. Ito, and N. Yamamoto, Exponentially accurate open quantum simulation via randomized dissipation with minimal ancilla, arXiv preprint arXiv:2412.19453 (2024).

[30] M. M. Taddei, B. M. Escher, L. Davidovich, and R. L. de Matos Filho, Quantum speed limit for physical processes, Physical review letters **110**, 050402 (2013).

[31] D. P. Pires, M. Cianciaruso, L. C. Céleri, G. Adesso, and D. O. Soares-Pinto, Generalized geometric quantum speed limits, Physical Review X **6**, 021031 (2016).

[32] S. Deffner and S. Campbell, Quantum speed limits: from heisenberg's uncertainty principle to optimal quantum control, Journal of Physics A: Mathematical and Theoretical **50**, 453001 (2017).

[33] J. D. Watson, Randomly compiled quantum simulation with exponentially reduced circuit depths, arXiv preprint arXiv:2411.04240 (2025).

[34] E. Bernstein and U. Vazirani, Quantum complexity theory, in *Proceedings of the twenty-fifth annual ACM symposium on Theory of computing* (1993) pp. 11–20.

[35] F. Verstraete, M. M. Wolf, and J. Ignacio Cirac, Quantum computation and quantum-state engineering driven by dissipation, Nature physics **5**, 633 (2009).

[36] C. Rouzé, D. S. França, and Á. M. Alhambra, Efficient thermalization and universal quantum computing with quantum gibbs samplers, in *Proceedings of the 57th Annual ACM Symposium on Theory of Computing* (2025) pp. 1488–1495.

[37] M. J. Kastoryano, M. M. Wolf, and J. Eisert, Precisely timing dissipative quantum information processing, Physical review letters **110**, 110501 (2013).

[38] W. M. Itano, D. J. Heinzen, J. J. Bollinger, and D. J. Wineland, Quantum zeno effect, Physical Review A **41**, 2295 (1990).

[39] P. Facchi and S. Pascazio, Quantum zeno subspaces, Physical review letters **89**, 080401 (2002).

[40] D. W. Berry, G. Ahokas, R. Cleve, and B. C. Sanders, Efficient quantum algorithms for simulating sparse hamiltonians, Communications in Mathematical Physics **270**, 359 (2007).

[41] Y. Atia and D. Aharonov, Fast-forwarding of hamiltonians and exponentially precise measurements, Nature communications **8**, 1572 (2017).

[42] E. Farhi, J. Goldstone, S. Gutmann, and M. Sipser, Limit on the speed of quantum computation in determining parity, Physical Review Letters **81**, 5442 (1998).

[43] M. Gao, Z. Ji, and C. Liu, Ancilla-free fast-forwarding lindbladian simulation algorithms by hamiltonian twirling, arXiv preprint arXiv:2511.10253 (2025).

[44] Z.-X. Shang, D. An, and C. Shao, Exponential lindbladian fast forwarding and exponential amplification of certain gibbs state properties, Reports on Progress in Physics (2025).

[45] P. Zanardi and L. Campos Venuti, Coherent quantum dynamics in steady-state manifolds of strongly dissipative systems, Physical review letters **113**, 240406 (2014).

[46] P. Zanardi and L. Campos Venuti, Geometry, robustness, and emerging unitarity in dissipation-projected dynamics, Phys-

ical Review A **91**, 052324 (2015).
[47] V. V. Albert, B. Bradlyn, M. Fraas, and L. Jiang, Geometry and response of lindbladians, Physical Review X **6**, 041031 (2016).
[48] J. Kempe, A. Kitaev, and O. Regev, The complexity of the local hamiltonian problem, Siam journal on computing **35**, 1070 (2006).
[49] H. Roger and R. J. Charles, Topics in matrix analysis (1994).

Appendix A: Proof of theorem 1 and related results

On $F = I - \delta A$: To avoid ambiguity, in the following, we will use $\|\cdot\|_\infty$ to represent the spectral norm $\|\cdot\|$ in the main text. When we set the jump operator to be $F = I - \delta A$ with $A = G + iH$, we have

$$\begin{aligned} F\rho F^\dagger &= (I - \delta(G+iH))\rho(I - \delta(G - iH)) \\ &= \rho - \delta(G+iH)\rho - \delta\rho(G-iH) + \delta^2(G+iH)\rho(G-iH) \\ &= \rho - \delta\{G,\rho\} - i\delta[H,\rho] + \delta^2(G+iH)\rho(G-iH). \end{aligned} \tag{A1}$$

Also, because we have

$$\begin{aligned} F^\dagger F &= (I - \delta(G-iH))(I - \delta(G+iH)) \\ &= I - \delta(G-iH) - \delta(G+iH) + \delta^2(G-iH)(G+iH) \\ &= I - 2\delta G + \delta^2(G-iH)(G+iH), \end{aligned} \tag{A2}$$

therefore, we have

$$\begin{aligned} \frac{1}{2}\{F^\dagger F, \rho\} &= \frac{1}{2}\{I - 2\delta G + \delta^2(G-iH)(G+iH), \rho\} \\ &= \rho - \delta\{G,\rho\} + \frac{1}{2}\delta^2\{(G-iH)(G+iH),\rho\}. \end{aligned} \tag{A3}$$

Thus, the derivative of the density matrix has the form

$$\begin{aligned} \frac{d\rho}{dt} &= \mathcal{D}_F[\rho] = F^\dagger\rho F - \frac{1}{2}\{F^\dagger F,\rho\} \\ &= \rho - \delta\{G,\rho\} - i\delta[H,\rho] + \delta^2(G+iH)\rho(G-iH) - \rho + \delta\{G,\rho\} - \frac{1}{2}\delta^2\{(G-iH)(G+iH),\rho\} \\ &= -i\delta[H,\rho] + \delta^2\mathcal{D}_A[\rho], \end{aligned} \tag{A4}$$

where we denote $\mathcal{D}_O[\rho] = O\rho O^\dagger - \frac{1}{2}\{O^\dagger O,\rho\}$.

Now, to bound the error of simulating the Hamiltonian dynamics, we first introduce the following lemma

Lemma 1. *Given two Lindbladians with the Liouvillian operators $\mathcal{L}_1$ and $\mathcal{L}_2$ respectively, the diamond distance between the two Lindbladians for an evolution time t has the upper bound*

$$\|e^{\mathcal{L}_1 t} - e^{\mathcal{L}_2 t}\|_\diamond \le t\|\mathcal{L}_1 - \mathcal{L}_2\|_\diamond. \tag{A5}$$

Proof. Using the Duhamel Identity [18], we have

$$e^{\mathcal{L}_1 t} - e^{\mathcal{L}_2 t} = \int_0^t e^{\mathcal{L}_2(t-s)}(\mathcal{L}_1 - \mathcal{L}_2)e^{\mathcal{L}_1 s}ds, \tag{A6}$$

which leads to

$$\begin{aligned} \|e^{\mathcal{L}_1 t} - e^{\mathcal{L}_2 t}\|_\diamond &\le \int_0^t \|e^{\mathcal{L}_2(t-s)}\|_\diamond\|\mathcal{L}_1 - \mathcal{L}_2\|_\diamond\|e^{\mathcal{L}_1 s}\|_\diamond ds \\ &\le \int_0^t \|\mathcal{L}_1 - \mathcal{L}_2\|_\diamond ds = t\|\mathcal{L}_1 - \mathcal{L}_2\|_\diamond, \end{aligned} \tag{A7}$$

where we use $\|e^{\mathcal{L}t}\|_\diamond \le 1$. □

Now, using lemma 1, we have

$$\|e^{\mathcal{D}_F t/\delta} - e^{\mathcal{L}_H t}\|_\diamond \leq t\delta \|\mathcal{D}_A\|_\diamond, \tag{A8}$$

where we use $\mathcal{L}_H$ to denote the Liouvillian operator of Hamiltonian dynamics under H. To have an approximation with an error ϵ, we can simply ask

$$t\delta\|\mathcal{D}_A\|_\diamond \leq \epsilon \to \delta \leq \frac{\epsilon}{t\|\mathcal{D}_A\|_\diamond}. \tag{A9}$$

Since the Lindbladian evolution time T is $T = t/\delta$, thus, we obtain

$$T \geq \|\mathcal{D}_A\|_\diamond t^2/\epsilon. \tag{A10}$$

Since $\|\mathcal{D}_A\|_\diamond = \mathcal{O}(\|A\|_\infty^2)$, we finish the proof

$$T = \mathcal{O}(\|A\|_\infty^2 t^2/\epsilon). \tag{A11}$$

When $A = iH$, we recover theorem 1.

On $F_i = I - i\delta H_i$: Similarly, when $H = \sum_i H_i$, and set jump operators $F_i = I - i\delta H_i$, we have

$$\begin{aligned}\frac{d\rho}{dt} &= \sum_i \mathcal{D}_{F_i}[\rho] = \sum_i \left(F_i^\dagger \rho F_i - \frac{1}{2}\{F_i^\dagger F_i, \rho\}\right) \\ &= -i\delta\left[\sum_i H_i, \rho\right] + \sum_i \delta^2 \mathcal{D}_{H_i}[\rho].\end{aligned} \tag{A12}$$

Using lemma 1, we have

$$\|e^{\sum_i \mathcal{D}_{F_i} t/\delta} - e^{\mathcal{L}_H t}\|_\diamond \leq t\delta \|\sum_i \mathcal{D}_{H_i}\|_\diamond \leq t\delta \sum_i \|\mathcal{D}_{H_i}\|_\diamond, \tag{A13}$$

which leads to

$$T = \mathcal{O}\left(\sum_i \|H_i\|_\infty^2 t^2/\epsilon\right). \tag{A14}$$

On General Lindbladian via dissipation: To simulate the general Lindbladian

$$\frac{d\rho}{dt} = \mathcal{L}[\rho] = -i[H, \rho] + \sum_i \left(F_i \rho F_i^\dagger - \frac{1}{2}\{\rho, F_i^\dagger F_i\}\right), \tag{A15}$$

via dissipation, we construct a purely dissipative Lindbladian $\mathcal{L}'$ with jumps $F_0' = I - i\delta H$ and $F_i' = \sqrt{\delta} F_i$. Since we have

$$\begin{aligned}\frac{d\rho}{dt} &= \mathcal{L}'[\rho] = F_0'^\dagger \rho F_0' - \frac{1}{2}\{F_0'^\dagger F_0', \rho\} + \sum_i \left(F_i'^\dagger \rho F_i' - \frac{1}{2}\{F_i'^\dagger F_i', \rho\}\right) \\ &= -i\delta[H, \rho] + \delta \sum_i \left(F_i^\dagger \rho F_i - \frac{1}{2}\{F_i^\dagger F_i, \rho\}\right) + \delta^2 \mathcal{D}_H[\rho] \\ &= \delta\mathcal{L}[\rho] + \delta^2 \mathcal{D}_H[\rho],\end{aligned} \tag{A16}$$

therefore, following the similar procedures as above, we obtain

$$T = \mathcal{O}\left(\|H\|_\infty^2 t^2/\epsilon\right). \tag{A17}$$

Appendix B: Proof of theorem 2

In this note we prove a rigorous lower bound under the *stronger* simulation requirement that the dissipative evolution must approximate the target Hamiltonian evolution *for every intermediate time* between 0 and t, not just at the final time. The result is proved for a simple qubit family, which is enough to establish the desired $\Omega(t^2/\epsilon)$ scaling in the worst-case sense.

a. Simulation notion. Let

$$\mathcal{L}_D(\rho) = \sum_{j=1}^{m} \left(F_j \rho F_j^\dagger - \tfrac{1}{2}\{F_j^\dagger F_j, \rho\} \right), \qquad \|F_j\|_\infty \le C, \tag{B1}$$

be a purely dissipative Lindbladian on a qubit, and let $\Phi_\tau = e^{\tau \mathcal{L}_D}$. For a target Hamiltonian H, define the unitary channel

$$\mathcal{U}_s(\rho) = e^{-iHs} \rho e^{iHs}. \tag{B2}$$

We say that Φ_τ simulates $\mathcal{U}_s$ up to time t in total dissipative time T if

$$\sup_{0 \le s \le t} \left\| \Phi_{\frac{T}{t}s} - \mathcal{U}_s \right\|_\diamond \le \epsilon. \tag{B3}$$

This is the natural uniform-in-time strengthening of the endpoint condition and matches the linear time reparametrization used by the constructive upper bound.

Theorem 3 (Uniform-in-time lower bound for a hard qubit family)**.** *Let*

$$H = \frac{\nu}{2}\sigma_z, \qquad \Theta := |\nu| t. \tag{B4}$$

Assume that (B3) *holds and that*

$$0 < \epsilon \le \frac{1}{100} \min\{1, \Theta\}. \tag{B5}$$

Then

$$T \ge \frac{\Theta^2}{384\, m C^2\, \epsilon} = \frac{\nu^2 t^2}{384\, m C^2\, \epsilon}. \tag{B6}$$

Equivalently, since $\|H\|_\infty = |\nu|/2$*,*

$$T \ge \frac{\|H\|_\infty^2 t^2}{96\, m C^2\, \epsilon}. \tag{B7}$$

In particular, for any fixed-norm hard family with $\|H\|_\infty = \Theta(1)$*, uniform-in-time pure-dissipative simulation requires*

$$T = \Omega(t^2/\epsilon). \tag{B8}$$

Proof. We write the qubit state as

$$\rho = \frac{1}{2}(I + \mathbf{r} \cdot \boldsymbol{\sigma}), \qquad \mathbf{r} \in \mathbb{R}^3, \tag{B9}$$

and represent channels in Bloch form.

b. Step 1: Bloch form of a purely dissipative qubit generator. Write each jump operator as

$$F_j = a_j I + \mathbf{u}_j \cdot \boldsymbol{\sigma}, \qquad a_j \in \mathbb{C}, \quad \mathbf{u}_j \in \mathbb{C}^3. \tag{B10}$$

A standard Pauli-basis calculation gives the affine Bloch equation [13]

$$\dot{\mathbf{r}} = B\mathbf{r} + \mathbf{c}, \qquad B = S + [\boldsymbol{\omega}\times], \tag{B11}$$

where $S = S^\top$ is real symmetric, $[\boldsymbol{\omega}\times]$ is the real antisymmetric matrix for the cross product by $\boldsymbol{\omega}$, and

$$S = 2\sum_{j=1}^{m} \Big(\mathrm{Re}(\mathbf{u}_j \mathbf{u}_j^\dagger) - |\mathbf{u}_j|^2 I_3 \Big), \tag{B12}$$

$$\boldsymbol{\omega} = -2\sum_{j=1}^{m} \mathrm{Im}(a_j^* \mathbf{u}_j). \tag{B13}$$

The translation vector $\mathbf{c}$ will not be needed explicitly.

Two consequences are immediate. First, $S \preceq 0$. Indeed, for every real $\mathbf{x} \in \mathbb{R}^3$,

$$\mathbf{x}^\top S\mathbf{x} = 2\sum_{j=1}^{m}\Big(|\mathbf{x}\cdot\mathbf{u}_j|^2 - |\mathbf{u}_j|^2|\mathbf{x}|^2\Big) \le 0. \tag{B14}$$

Hence

$$\|S\|_\infty \le -\mathrm{Tr}(S). \tag{B15}$$

Second, taking the trace in (B12) gives

$$-\mathrm{Tr}(S) = 4\sum_{j=1}^{m}|\mathbf{u}_j|^2. \tag{B16}$$

Using $|a_j| \le \|F_j\|_\infty \le C$ and Cauchy–Schwarz,

$$|\boldsymbol{\omega}| \le 2\sum_{j=1}^{m}|a_j|\,|\mathbf{u}_j| \le 2C\sqrt{m\sum_{j=1}^{m}|\mathbf{u}_j|^2} \tag{B17}$$

$$= C\sqrt{m(-\mathrm{Tr}S)}, \tag{B18}$$

where the last equality uses (B16). Thus

$$|\boldsymbol{\omega}|^2 \le mC^2(-\mathrm{Tr}S). \tag{B19}$$

c. Step 2: Uniform channel closeness implies uniform Bloch-matrix closeness. Let $A_\tau = e^{\tau B}$ denote the linear part of Φ_τ in Bloch form, so that

$$\mathbf{r} \mapsto A_\tau\mathbf{r} + \mathbf{b}_\tau. \tag{B20}$$

The target channel generated by $H = \frac{\nu}{2}\sigma_z$ acts on Bloch vectors by the rotation

$$R_z(\alpha\tau), \qquad \alpha := \frac{\nu t}{T} = \frac{\Theta}{T}. \tag{B21}$$

Since the trace distance between qubit states equals the Euclidean distance between their Bloch vectors, (B3) implies that for every unit vector $\mathbf{r} \in \mathbb{R}^3$ and every $\tau \in [0,T]$,

$$\big|A_\tau\mathbf{r} + \mathbf{b}_\tau - R_z(\alpha\tau)\mathbf{r}\big| \le \epsilon. \tag{B22}$$

Applying (B22) to both $\mathbf{r}$ and $-\mathbf{r}$ and adding/subtracting the two inequalities yields

$$\|A_\tau - R_z(\alpha\tau)\|_\infty \le \epsilon, \qquad |\mathbf{b}_\tau| \le \epsilon, \qquad 0 \le \tau \le T. \tag{B23}$$

d. Step 3: Uniform closeness forces very small total contraction. Taking $\tau = T$ in (B23), Weyl's inequality [49] for singular values implies that every singular value of A_T lies in $[1-\epsilon, 1+\epsilon]$, because all singular values of the rotation $R_z(\Theta)$ are equal to 1. Therefore

$$\det(A_T) \ge (1-\epsilon)^3. \tag{B24}$$

Since $A_T = e^{TB}$ and $\mathrm{Tr}([\boldsymbol{\omega}\times]) = 0$,

$$\det(A_T) = e^{T\mathrm{Tr}(B)} = e^{T\mathrm{Tr}(S)}. \tag{B25}$$

Hence, for $\epsilon \le 1/2$,

$$-\mathrm{Tr}(S) \le \frac{3}{T}\log\frac{1}{1-\epsilon} \le \frac{6\epsilon}{T}. \tag{B26}$$

By (B15),

$$\|S\|_\infty \le \frac{6\epsilon}{T}. \tag{B27}$$

e. Step 4: Uniform closeness to the rotating orbit forces a macroscopic path length. Let

$$\mathbf{u}(\tau) := R_z(\alpha\tau)\mathbf{e}_x, \qquad \mathbf{v}(\tau) := A_\tau \mathbf{e}_x, \tag{B28}$$

where $\mathbf{e}_x = (1,0,0)^\top$. By (B23),

$$|\mathbf{v}(\tau) - \mathbf{u}(\tau)| \le \epsilon, \qquad 0 \le \tau \le T. \tag{B29}$$

We claim that the Euclidean arc length $L(\mathbf{v})$ of $\mathbf{v}(\tau)$ satisfies

$$L(\mathbf{v}) \ge \frac{\Theta}{5}. \tag{B30}$$

Indeed:

Case 1: $0 < \Theta \le 1$. Since length dominates endpoint distance,

$$L(\mathbf{v}) \ge |\mathbf{v}(T) - \mathbf{v}(0)| \ge |\mathbf{u}(T) - \mathbf{u}(0)| - 2\epsilon \tag{B31}$$

$$= 2\sin(\Theta/2) - 2\epsilon \ge \Theta/2 - 2\epsilon \ge \Theta/4, \tag{B32}$$

where in the last step we used (B5).

Case 2: $\Theta \ge 1$. Let $N = \lfloor \Theta \rfloor$, so $N \ge \Theta/2$. For $k = 0, 1, \ldots, N$, define $\tau_k = k/\alpha$. Then consecutive target points are separated by one radian, hence

$$|\mathbf{u}(\tau_{k+1}) - \mathbf{u}(\tau_k)| = 2\sin(1/2) > 0.95. \tag{B33}$$

Using (B29) and (B5),

$$|\mathbf{v}(\tau_{k+1}) - \mathbf{v}(\tau_k)| \ge |\mathbf{u}(\tau_{k+1}) - \mathbf{u}(\tau_k)| - 2\epsilon > 0.93. \tag{B34}$$

Therefore

$$L(\mathbf{v}) \ge \sum_{k=0}^{N-1} |\mathbf{v}(\tau_{k+1}) - \mathbf{v}(\tau_k)| > 0.93N \ge 0.46\Theta > \frac{\Theta}{5}. \tag{B35}$$

This proves (B30).

f. Step 5: Convert path length into a lower bound on the effective rotation rate. Since $\dot{\mathbf{v}}(\tau) = B\mathbf{v}(\tau)$, we have

$$L(\mathbf{v}) = \int_0^T |\dot{\mathbf{v}}(\tau)|\, d\tau \le \int_0^T \|B\|_\infty\, |\mathbf{v}(\tau)|\, d\tau \tag{B36}$$

$$\le (1+\epsilon)T\big(|\boldsymbol{\omega}| + \|S\|_\infty\big), \tag{B37}$$

where we used $\|[\boldsymbol{\omega}\times]\|_\infty = |\boldsymbol{\omega}|$ and $|\mathbf{v}(\tau)| \le |\mathbf{u}(\tau)| + \epsilon = 1 + \epsilon$. Combining (B30), (B37), and (B27), we obtain

$$|\boldsymbol{\omega}| \ge \frac{\Theta}{5(1+\epsilon)T} - \frac{6\epsilon}{T}. \tag{B38}$$

Under (B5), the second term is at most $0.06\,\Theta/T$ and the first term is at least $0.19\,\Theta/T$, so in particular

$$|\boldsymbol{\omega}| \ge \frac{\Theta}{8T}. \tag{B39}$$

g. Step 6: Finish the lower bound. Combining (B39), (B19), and (B26), we find

$$\frac{\Theta^2}{64T^2} \le |\boldsymbol{\omega}|^2 \le mC^2(-\mathrm{Tr}S) \le \frac{6mC^2\epsilon}{T}. \tag{B40}$$

Rearranging gives

$$T \ge \frac{\Theta^2}{384\, mC^2\, \epsilon}, \tag{B41}$$

which is exactly (B6). □

Appendix C: Uniqueness of construction for smooth Lindbladians

In this section we discuss to what extent our construction is unique, showing that any smooth family of semigroups that can approximate Hamiltonian dynamics to arbitrary precision (potentially at the cost of increased simulation time), must have a form similar to our evolution up to second order.

Proposition 2 (Uniqueness up to $O(\delta^2)$)**.** *Let $\{\mathcal{L}_{D,\delta}\}_{0\le\delta<\delta_0}$ be a smooth family of purely dissipative Lindbladians on a finite-dimensional system, and let*

$$\mathcal{L}_H(\rho) := -i[H,\rho]. \tag{C1}$$

Assume that there exists $t_0 > 0$ such that

$$\varepsilon(\delta) := \sup_{0\le s\le t_0} \left\| e^{\frac{s}{\delta}\mathcal{L}_{D,\delta}} - e^{s\mathcal{L}_H} \right\|_\diamond \xrightarrow[\delta\to 0]{} 0. \tag{C2}$$

Then

$$\mathcal{L}_{D,\delta} = \delta\mathcal{L}_H + O(\delta^2) \tag{C3}$$

in diamond norm. In particular, the first-order term is uniquely fixed by H. Equivalently, if $\widetilde{\mathcal{L}}_{D,\delta}$ is another smooth purely dissipative family satisfying (C2) for the same Hamiltonian H, then

$$\mathcal{L}_{D,\delta} - \widetilde{\mathcal{L}}_{D,\delta} = O(\delta^2). \tag{C4}$$

Moreover, assume that for some fixed m one can choose jump operators smoothly so that

$$\mathcal{L}_{D,\delta}(\rho) = \sum_{j=1}^{m} \left(F_{j,\delta}\rho F_{j,\delta}^\dagger - \frac{1}{2}\{F_{j,\delta}^\dagger F_{j,\delta}, \rho\} \right), \qquad F_{j,\delta} = F_{j,0} + \delta G_j + O(\delta^2). \tag{C5}$$

Then $F_{j,0} = c_j I$ for some scalars c_j, and

$$H = \sum_{j=1}^{m} \frac{c_j G_j^\dagger - c_j^* G_j}{2i}. \tag{C6}$$

Hence, modulo the usual Lindblad gauge freedom and up to $O(\delta^2)$, every nontrivial first-order jump has the form

$$F_{j,\delta} = \sqrt{\gamma_j}\big(I - \delta A_j\big) + O(\delta^2), \qquad \sum_j \gamma_j \frac{A_j - A_j^\dagger}{2i} = H, \tag{C7}$$

while jumps with $F_{j,0} = 0$ contribute only at order $O(\delta^2)$.

Proof. Set

$$\Phi_{\delta,s} := e^{\frac{s}{\delta}\mathcal{L}_{D,\delta}}, \qquad U_s := e^{s\mathcal{L}_H}. \tag{C8}$$

We first show that $\mathcal{L}_{D,0} = 0$. Fix any $a > 0$. For all sufficiently small δ, we have $a\delta \le t_0$, and therefore (C2) implies

$$\left\| e^{a\mathcal{L}_{D,\delta}} - e^{a\delta\mathcal{L}_H} \right\|_\diamond \le \varepsilon(\delta). \tag{C9}$$

Now let $\delta \to 0$. Since $\mathcal{L}_{D,\delta}$ is smooth at $\delta = 0$, we get

$$e^{a\mathcal{L}_{D,0}} = I. \tag{C10}$$

Since this holds for every $a > 0$, differentiating at $a = 0$ yields

$$\mathcal{L}_{D,0} = 0. \tag{C11}$$

Because the family is smooth, there exists a bounded superoperator $\mathcal{M}$ such that

$$\mathcal{L}_{D,\delta} = \delta\mathcal{M} + O(\delta^2), \qquad \mathcal{M} = \partial_\delta \mathcal{L}_{D,\delta}\big|_{\delta=0}. \tag{C12}$$

Define

$$A_\delta := \delta^{-1}\mathcal{L}_{D,\delta} = \mathcal{M} + O(\delta). \tag{C13}$$

By Duhamel's formula,

$$e^{sA_\delta} - e^{s\mathcal{M}} = \int_0^s e^{(s-u)A_\delta}(A_\delta - \mathcal{M})e^{u\mathcal{M}}\,du. \tag{C14}$$

Hence, for $0 \le s \le t_0$,

$$\begin{aligned}\|e^{sA_\delta} - e^{s\mathcal{M}}\|_\diamond &\le s\, e^{s(\|A_\delta\|_\diamond + \|\mathcal{M}\|_\diamond)}\|A_\delta - \mathcal{M}\|_\diamond \\ &= O(\delta),\end{aligned} \tag{C15}$$

uniformly on $[0, t_0]$. Since $e^{sA_\delta} = e^{\frac{s}{\delta}\mathcal{L}_{D,\delta}}$, combining this with (C2) gives

$$\sup_{0\le s\le t_0} \|e^{s\mathcal{M}} - e^{s\mathcal{L}_H}\|_\diamond \le \|e^{s\mathcal{M}} - e^{\frac{s}{\delta}\mathcal{L}_{D,\delta}}\|_\diamond + \|e^{\frac{s}{\delta}\mathcal{L}_{D,\delta}} - e^{s\mathcal{L}_H}\|_\diamond = O(\delta + \epsilon(\delta)). \tag{C16}$$

Letting $\delta \to 0$ we conclude that:

$$\sup_{0\le s\le t_0} \|e^{s\mathcal{M}} - e^{s\mathcal{L}_H}\|_\diamond = 0. \tag{C17}$$

Therefore

$$e^{s\mathcal{M}} = e^{s\mathcal{L}_H} \qquad \text{for all } 0 \le s \le t_0. \tag{C18}$$

Differentiating at $s = 0$ yields

$$\mathcal{M} = \mathcal{L}_H. \tag{C19}$$

This proves (C3).

We now prove the jump statement. Write

$$\mathcal{D}_F(\rho) := F\rho F^\dagger - \frac{1}{2}\{F^\dagger F, \rho\}, \qquad \mathcal{L}_{D,\delta} = \sum_{j=1}^m \mathcal{D}_{F_{j,\delta}}. \tag{C20}$$

Since $\mathcal{L}_{D,0} = 0$, we have

$$0 = \mathcal{L}_{D,0} = \sum_{j=1}^m \mathcal{D}_{F_{j,0}}. \tag{C21}$$

Let $\rho = |\psi\rangle\langle\psi|$ be pure. Then

$$\begin{aligned}0 &= \mathrm{Tr}(\rho\,\mathcal{L}_{D,0}[\rho]) \\ &= -\sum_{j=1}^m \left(\langle\psi|F_{j,0}^\dagger F_{j,0}|\psi\rangle - |\langle\psi|F_{j,0}|\psi\rangle|^2\right).\end{aligned} \tag{C22}$$

Each summand is nonnegative, so every summand must vanish for every $|\psi\rangle$. Hence each $F_{j,0}$ has zero variance on every pure state, which implies

$$F_{j,0} = c_j I \tag{C23}$$

for some scalar c_j.

Now write

$$F_{j,\delta} = c_j I + \delta G_j + O(\delta^2). \tag{C24}$$

A direct expansion gives

$$\mathcal{D}_{F_{j,\delta}}[\rho] = \delta\left(c_j^* G_j \rho + c_j \rho G_j^\dagger - \frac{1}{2}\{c_j G_j^\dagger + c_j^* G_j, \rho\}\right) + O(\delta^2)$$
$$= -i\delta\left[\frac{c_j G_j^\dagger - c_j^* G_j}{2i}, \rho\right] + O(\delta^2). \tag{C25}$$

Summing (C25) over j and comparing with (C3) proves

$$H = \sum_{j=1}^{m} \frac{c_j G_j^\dagger - c_j^* G_j}{2i}, \tag{C26}$$

which is (C6).

Finally, if $c_j \neq 0$, write

$$G_j = -c_j A_j, \tag{C27}$$

so that

$$F_{j,\delta} = c_j(I - \delta A_j) + O(\delta^2). \tag{C28}$$

The overall phase of c_j is irrelevant because $\mathcal{D}_{e^{i\theta}F} = \mathcal{D}_F$. Thus, after removing the phase and defining $\gamma_j := |c_j|^2$, we may rewrite

$$F_{j,\delta} = \sqrt{\gamma_j}(I - \delta A_j) + O(\delta^2). \tag{C29}$$

Then (C6) becomes

$$\sum_j \gamma_j \frac{A_j - A_j^\dagger}{2i} = H. \tag{C30}$$

If $c_j = 0$, then $F_{j,\delta} = O(\delta)$ and hence

$$\mathcal{D}_{F_{j,\delta}} = O(\delta^2), \tag{C31}$$

so such jumps do not contribute at first order. This proves (C7). □

Appendix D: Autonomous qDRIFT from displaced Pauli channels

We now transform the results of the last sections into a concrete measurement-native primitive. The relevant situation is a platform in which Pauli products are available as readout or loss channels, but are costly to implement as coherent many-body Hamiltonian interactions. In such a platform, a coherent displacement of the parity channel produces precisely the nontraceless jump operators needed above. In particular, we will show how to obtain an autonomous version of QDRIFT [15] in our framework.

qDRIFT seems a natural target for our technique, as it corresponds to a randomized approximate simulation of Hamiltonian simulation. More precisely, QDRIFT performs randomized Hamiltonian simulation by sampling Pauli terms with probabilities proportional to their coefficients [15]. The construction below realizes a continuous-time, measurement-native analogue of qDRIFT. The random scheduler is not a classical compiler; it is the bath itself. At the operating point used for Hamiltonian simulation, the click record is state-independent, so the unconditional channel is generated without outcome-conditioned feedback. The price is the same sampling diffusion that appears in Poissonized qDRIFT, here written as measurement shot noise.

Thus, our claim is that if a Pauli operator P is native as a displaced readout/backaction channel, then the unconditional backaction of that channel implements an approximate Hamiltonian term proportional to P.

1. Displaced counting instruments and their Markovian limit

We first define precisely what is meant by a displaced Pauli channel. Let $\mathcal{H}$ be a finite-dimensional system Hilbert space. Given system operators

$$F_1, \dots, F_L \in \mathcal{B}(\mathcal{H}),$$

define

$$M := \sum_{\ell=1}^{L} F_\ell^\dagger F_\ell. \tag{D1}$$

For a small time step $\eta > 0$ satisfying

$$0 \le \eta M \le I, \tag{D2}$$

define the $(L+1)$-outcome weak counting instrument with Kraus operators

$$K_0(\eta) := (I - \eta M)^{1/2}, \qquad K_\ell(\eta) := \sqrt{\eta}\, F_\ell, \qquad \ell = 1, \dots, L. \tag{D3}$$

The outcome 0 is the no-click outcome, while outcome $\ell \ge 1$ is a click in channel ℓ. The instrument is trace preserving because

$$K_0(\eta)^\dagger K_0(\eta) + \sum_{\ell=1}^{L} K_\ell(\eta)^\dagger K_\ell(\eta) = I. \tag{D4}$$

After discarding the classical record, the one-step channel is

$$\Phi_\eta(\rho) := K_0(\eta)\rho K_0(\eta) + \eta \sum_{\ell=1}^{L} F_\ell \rho F_\ell^\dagger. \tag{D5}$$

Lemma 2 (Markovian limit of the counting instrument)**.** *Let*

$$\mathcal{L}[\rho] := \sum_{\ell=1}^{L} \left(F_\ell \rho F_\ell^\dagger - \frac{1}{2}\{F_\ell^\dagger F_\ell, \rho\} \right). \tag{D6}$$

Then

$$\Phi_\eta = \mathrm{id} + \eta\mathcal{L} + O(\eta^2) \tag{D7}$$

in diamond norm. Consequently, for every fixed $\tau \ge 0$,

$$\lim_{n\to\infty} \Phi_{\tau/n}^n = e^{\tau\mathcal{L}} \tag{D8}$$

in diamond norm.

Proof. Since $\mathcal{H}$ is finite dimensional, the functional calculus expansion of the square root gives

$$(I - \eta M)^{1/2} = I - \frac{\eta}{2} M + O(\eta^2) \tag{D9}$$

in operator norm. Substituting this into eq. (D5) gives

$$\Phi_\eta(\rho) = \left(I - \frac{\eta}{2}M\right) \rho \left(I - \frac{\eta}{2}M\right) + \eta \sum_\ell F_\ell \rho F_\ell^\dagger + O(\eta^2) \tag{D10}$$

$$= \rho + \eta \sum_\ell \left(F_\ell \rho F_\ell^\dagger - \frac{1}{2}\{F_\ell^\dagger F_\ell, \rho\} \right) + O(\eta^2). \tag{D11}$$

This proves eq. (D7). The product-formula limit eq. (D8) follows from the Chernoff theorem, or directly from the finite-dimensional estimate

$$\left\| \left(I + \frac{\tau}{n}\mathcal{L} + O(n^{-2})\right)^n - e^{\tau\mathcal{L}} \right\|_\diamond \to 0.$$

□

Thus specifying a weak counting instrument with jump amplitudes F_ℓ is equivalent, in the continuous-time limit, to specifying the Lindbladian $\sum_\ell \mathcal{D}_{F_\ell}$. This is the mathematical sense in which the dissipators used below are constructed from measurement channels.

2. Displacing a Pauli-product channel

Let $P = P^\dagger$ be a Pauli product, so $P^2 = I$. A displaced Pauli counting channel is a weak counting channel whose jump amplitude is

$$F = \alpha I + \beta P, \qquad \alpha, \beta \in \mathbb{C}. \tag{D12}$$

Let

$$\Pi_\pm := \frac{I \pm P}{2} \tag{D13}$$

be the parity projectors. Then

$$F = (\alpha + \beta)\Pi_+ + (\alpha - \beta)\Pi_-. \tag{D14}$$

Thus a click multiplies the two parity sectors by different complex amplitudes. The magnitudes of these amplitudes determine information gain about P, while their relative phase determines coherent phase backaction.

The click effect is

$$F^\dagger F = (|\alpha|^2 + |\beta|^2)I + 2\mathrm{Re}(\alpha^*\beta)P. \tag{D15}$$

Hence, in a time step η, the click probability is

$$p_{\mathrm{click}}(\rho) = \eta \mathrm{Tr}(F^\dagger F \rho) = \eta \left(|\alpha|^2 + |\beta|^2 + 2\mathrm{Re}(\alpha^*\beta)\mathrm{Tr}(P\rho) \right). \tag{D16}$$

The real part of $\alpha^*\beta$ is the information-bearing quadrature. The imaginary part is the Hamiltonian-generating quadrature.

Lemma 3 (Displaced Pauli dissipator)**.** *For $P = P^\dagger$, $P^2 = I$, and $F = \alpha I + \beta P$,*

$$\mathcal{D}_{\alpha I + \beta P}[\rho] = -i[-Im(\alpha^*\beta)P, \rho] + |\beta|^2(P\rho P - \rho). \tag{D17}$$

Proof. Using $P = P^\dagger$ and $P^2 = I$,

$$F\rho F^\dagger = |\alpha|^2\rho + \alpha\beta^*\rho P + \alpha^*\beta P\rho + |\beta|^2 P\rho P, \tag{D18}$$

$$F^\dagger F = (|\alpha|^2 + |\beta|^2)I + (\alpha^*\beta + \alpha\beta^*)P. \tag{D19}$$

Writing $z = \alpha^*\beta$, the cross term in the dissipator is

$$zP\rho + z^*\rho P - \frac{1}{2}(z + z^*)(P\rho + \rho P) = i\,\mathrm{Im}(z)(P\rho - \rho P) \tag{D20}$$

$$= i\,\mathrm{Im}(\alpha^*\beta)[P, \rho]. \tag{D21}$$

Combining this with the $|\beta|^2$ term gives eq. (D17). □

The phase-backaction operating point is obtained by choosing $\mathrm{Re}(\alpha^*\beta) = 0$. Then the click probability is independent of $\mathrm{Tr}(P\rho)$, while the dissipator still contains a Hamiltonian commutator. This is the regime used for Hamiltonian simulation.

For later use, it is convenient to introduce a weighted version. For a Pauli term hP, a channel-strength parameter $\gamma > 0$, a small parameter $\delta > 0$, and a sign $\sigma \in \{+1, -1\}$, define

$$F^{(\sigma)}_{\delta,\gamma,h,P} := \sqrt{\gamma}\, I - i\sigma\delta\frac{h}{\sqrt{\gamma}}P. \tag{D22}$$

This is a displaced Pauli jump with

$$\alpha = \sqrt{\gamma}, \qquad \beta = -i\sigma\delta\frac{h}{\sqrt{\gamma}}. \tag{D23}$$

Its click effect is scalar:

$$\left(F^{(\sigma)}_{\delta,\gamma,h,P}\right)^\dagger F^{(\sigma)}_{\delta,\gamma,h,P} = \left(\gamma + \delta^2\frac{h^2}{\gamma}\right) I. \tag{D24}$$

Therefore the associated weak counting channel carries no information about the eigenvalue of P at this operating point.

Equivalently, the same jump admits the polar decomposition

$$F^{(\sigma)}_{\delta,\gamma,h,P} = \sqrt{\gamma + \delta^2 h^2/\gamma}\, \exp\left[-i\sigma \arctan\left(\frac{\delta h}{\gamma}\right) P\right]. \tag{D25}$$

Thus the corresponding quantum trajectory is a Poisson process of small Pauli rotations. The deterministic Hamiltonian drift is the mean phase backaction; the residual dephasing is the shot noise of the random jump times.

3. Weighted displaced channels for a Pauli Hamiltonian

Let

$$H = \sum_{\ell=1}^{L} h_\ell P_\ell, \qquad h_\ell \in \mathbb{R}, \qquad P_\ell = P_\ell^\dagger, \qquad P_\ell^2 = I, \tag{D26}$$

where the Pauli strings P_ℓ need not commute. For each nonzero coefficient h_ℓ, choose a positive channel strength $\gamma_\ell > 0$. Define

$$F^{(\sigma)}_{\ell,\delta} := \sqrt{\gamma_\ell}\, I - i\sigma\delta \frac{h_\ell}{\sqrt{\gamma_\ell}} P_\ell, \qquad \sigma \in \{+1, -1\}. \tag{D27}$$

The sign $\sigma = +1$ generates $+H$, while $\sigma = -1$ generates $-H$. We write

$$\mathcal{L}_A[\rho] := -i[A, \rho], \qquad \mathcal{Z}_P[\rho] := P\rho P - \rho. \tag{D28}$$

Lemma 4 (Weighted displaced-Pauli identity)**.** *For $F^{(\sigma)}_{\ell,\delta}$ in eq. (D27),*

$$\mathcal{D}_{F^{(\sigma)}_{\ell,\delta}}[\rho] = \sigma\delta\, \mathcal{L}_{h_\ell P_\ell}[\rho] + \delta^2 \frac{h_\ell^2}{\gamma_\ell} \mathcal{Z}_{P_\ell}[\rho]. \tag{D29}$$

Moreover,

$$\left(F^{(\sigma)}_{\ell,\delta}\right)^\dagger F^{(\sigma)}_{\ell,\delta} = r_{\ell,\delta} I, \qquad r_{\ell,\delta} := \gamma_\ell + \delta^2 \frac{h_\ell^2}{\gamma_\ell}. \tag{D30}$$

Thus the click effect of every channel is proportional to the identity.

Proof. This is lemma 3 with

$$\alpha = \sqrt{\gamma_\ell}, \qquad \beta = -i\sigma\delta \frac{h_\ell}{\sqrt{\gamma_\ell}}.$$

Then

$$\mathrm{Im}(\alpha^* \beta) = -\sigma\delta h_\ell, \qquad |\beta|^2 = \delta^2 h_\ell^2/\gamma_\ell,$$

which gives eq. (D29). The scalar-effect identity follows from $P_\ell^2 = I$. □

The full weak counting instrument for the Pauli Hamiltonian is obtained by taking the jump amplitudes in eq. (D27). Its effect operator is

$$M_{\delta,\gamma} := \sum_{\ell=1}^{L} \left(F^{(\sigma)}_{\ell,\delta}\right)^\dagger F^{(\sigma)}_{\ell,\delta} = \Lambda_{\delta,\gamma} I, \qquad \Lambda_{\delta,\gamma} := \sum_{\ell=1}^{L} \left(\gamma_\ell + \delta^2 \frac{h_\ell^2}{\gamma_\ell}\right). \tag{D31}$$

Consequently, for any time step

$$0 < \eta \le \Lambda_{\delta,\gamma}^{-1},$$

the no-click Kraus operator is simply

$$K_0(\eta) = \sqrt{1 - \eta\Lambda_{\delta,\gamma}}\, I, \tag{D32}$$

while

$$K_\ell(\eta) = \sqrt{\eta}\, F^{(\sigma)}_{\ell,\delta}. \tag{D33}$$

Thus neither the click probabilities nor the no-click evolution reveal information about the system state. The record is a classical Poisson record of kick times and labels.

Define the purely dissipative generator

$$\mathcal{L}^{(\sigma)}_{\delta,\gamma} := \sum_{\ell=1}^{L} \mathcal{D}_{F^{(\sigma)}_{\ell,\delta}}. \tag{D34}$$

By lemma 4,

$$\mathcal{L}^{(\sigma)}_{\delta,\gamma} = \sigma\delta\mathcal{L}_H + \delta^2\mathcal{R}_\gamma, \tag{D35}$$

where

$$\mathcal{R}_\gamma := \sum_{\ell=1}^{L} \frac{h_\ell^2}{\gamma_\ell}\mathcal{Z}_{P_\ell}. \tag{D36}$$

Since $\rho \mapsto P_\ell \rho P_\ell$ is a unitary channel,

$$\|\mathcal{Z}_{P_\ell}\|_\diamond = \|P_\ell(\cdot)P_\ell - \mathrm{id}\,\|_\diamond \le 2. \tag{D37}$$

Therefore

$$\|\mathcal{R}_\gamma\|_\diamond \le 2S_\gamma, \qquad S_\gamma := \sum_{\ell=1}^{L} \frac{h_\ell^2}{\gamma_\ell}. \tag{D38}$$

Proposition 3 (Weighted displaced-Pauli simulation)**.** *For every $t \ge 0$,*

$$\sup_{0\le s\le t} \left\| e^{(s/\delta)\mathcal{L}^{(+)}_{\delta,\gamma}} - e^{s\mathcal{L}_H} \right\|_\diamond \le 2t\delta S_\gamma. \tag{D39}$$

Consequently, choosing

$$0 < \delta \le \frac{\epsilon}{2tS_\gamma} \tag{D40}$$

gives diamond-norm error at most ϵ, with dissipative evolution time

$$T = \frac{t}{\delta} = O\left(\frac{t^2}{\epsilon}\sum_{\ell=1}^{L}\frac{h_\ell^2}{\gamma_\ell}\right). \tag{D41}$$

Proof. By eq. (D35),

$$\frac{1}{\delta}\mathcal{L}^{(+)}_{\delta,\gamma} = \mathcal{L}_H + \delta\mathcal{R}_\gamma. \tag{D42}$$

Thus

$$e^{(s/\delta)\mathcal{L}^{(+)}_{\delta,\gamma}} = e^{s(\mathcal{L}_H + \delta\mathcal{R}_\gamma)}. \tag{D43}$$

Duhamel's identity gives

$$e^{s(\mathcal{L}_H+\delta\mathcal{R}_\gamma)} - e^{s\mathcal{L}_H} = \int_0^s e^{(s-u)(\mathcal{L}_H+\delta\mathcal{R}_\gamma)}\delta\mathcal{R}_\gamma e^{u\mathcal{L}_H}\, du. \tag{D44}$$

Both semigroups in the integrand are completely positive and trace preserving, hence have diamond norm one. Therefore

$$\left\| e^{s(\mathcal{L}_H+\delta\mathcal{R}_\gamma)} - e^{s\mathcal{L}_H} \right\|_\diamond \le s\delta\|\mathcal{R}_\gamma\|_\diamond \tag{D45}$$

$$\le 2s\delta S_\gamma \le 2t\delta S_\gamma. \tag{D46}$$

□

4. Optimal rates and exact Poissonized qDRIFT

The weights γ_ℓ are physical channel strengths. Fix the total available displaced-channel strength

$$\Gamma := \sum_{\ell=1}^{L} \gamma_\ell, \tag{D47}$$

and define

$$\lambda := \sum_{\ell=1}^{L} |h_\ell|. \tag{D48}$$

Terms with $h_\ell = 0$ are omitted. The optimal rate allocation is

$$\gamma_\ell^\star = \Gamma \frac{|h_\ell|}{\lambda}. \tag{D49}$$

Lemma 5 (Optimal channel allocation)**.** *Among all $\gamma_\ell > 0$ satisfying $\sum_\ell \gamma_\ell = \Gamma$, the quantity*

$$S_\gamma = \sum_{\ell=1}^{L} \frac{h_\ell^2}{\gamma_\ell} \tag{D50}$$

is minimized by eq. (D49). The minimum is

$$S_{\gamma^\star} = \frac{\lambda^2}{\Gamma}. \tag{D51}$$

Proof. By Cauchy–Schwarz,

$$\lambda^2 = \left(\sum_\ell |h_\ell| \right)^2 \tag{D52}$$

$$= \left(\sum_\ell \sqrt{\gamma_\ell} \frac{|h_\ell|}{\sqrt{\gamma_\ell}} \right)^2 \tag{D53}$$

$$\leq \left(\sum_\ell \gamma_\ell \right) \left(\sum_\ell \frac{h_\ell^2}{\gamma_\ell} \right) = \Gamma S_\gamma. \tag{D54}$$

Thus $S_\gamma \geq \lambda^2/\Gamma$. Equality holds exactly when $\gamma_\ell \propto |h_\ell|$, giving eq. (D49). □

At the optimal allocation the correspondence with qDRIFT becomes exact at the semigroup level. Let

$$s_\ell := \operatorname{sgn}(h_\ell), \qquad x := \frac{\delta\lambda}{\Gamma}, \qquad \theta := \arctan x. \tag{D55}$$

Then

$$F_{\ell,\delta}^{(+)} = \sqrt{\gamma_\ell^\star}\, (I - ixs_\ell P_\ell) = \sqrt{r_{\ell,\delta}}\, U_{\ell,\delta}, \tag{D56}$$

where

$$r_{\ell,\delta} = \gamma_\ell^\star (1 + x^2), \qquad U_{\ell,\delta} = e^{-i\theta s_\ell P_\ell}. \tag{D57}$$

The total jump rate is

$$\Lambda_\delta := \sum_\ell r_{\ell,\delta} = \Gamma(1 + x^2). \tag{D58}$$

Conditioned on a jump, the label distribution is

$$p_\ell = \frac{r_{\ell,\delta}}{\Lambda_\delta} = \frac{|h_\ell|}{\lambda}. \tag{D59}$$

Thus the bath samples the same Pauli labels as qDRIFT.

Theorem 4 (Exact autonomous qDRIFT semigroup)**.** *With the optimal allocation $\gamma^\star_\ell$, the rescaled dissipative generator has the exact mixed-unitary form*

$$\frac{1}{\delta}\mathcal{L}^{(+)}_{\delta,\gamma^\star} = \frac{\Lambda_\delta}{\delta}\sum_{\ell=1}^{L} p_\ell \left(U_{\ell,\delta}(\cdot)U^\dagger_{\ell,\delta} - \mathrm{id}\right), \tag{D60}$$

where

$$p_\ell = \frac{|h_\ell|}{\lambda}, \qquad U_{\ell,\delta} = e^{-i\theta s_\ell P_\ell}, \qquad \theta = \arctan\left(\frac{\delta\lambda}{\Gamma}\right). \tag{D61}$$

Equivalently,

$$\frac{1}{\delta}\mathcal{L}^{(+)}_{\delta,\gamma^\star} = \mathcal{L}_H + \frac{\delta\lambda}{\Gamma}\sum_{\ell=1}^{L}|h_\ell|\mathcal{Z}_{P_\ell}. \tag{D62}$$

Thus the displaced-channel dephasing is exactly the Poissonized qDRIFT diffusion term.

Proof. Since

$$F^{(+)}_{\ell,\delta} = \sqrt{r_{\ell,\delta}}\, U_{\ell,\delta}, \tag{D63}$$

we have

$$\mathcal{D}_{F^{(+)}_{\ell,\delta}}[\rho] = r_{\ell,\delta}\left(U_{\ell,\delta}\rho U^\dagger_{\ell,\delta} - \rho\right). \tag{D64}$$

Summing over ℓ, dividing by δ, and using $r_{\ell,\delta}/\Lambda_\delta = p_\ell$ proves eq. (D60).

It remains to verify eq. (D62). For a Hermitian involution P,

$$e^{-i\theta P}\rho e^{i\theta P} - \rho = -i\sin\theta\cos\theta[P,\rho] + \sin^2\theta(P\rho P - \rho). \tag{D65}$$

Applying this with $P = s_\ell P_\ell$, and using

$$\sin\theta\cos\theta = \frac{x}{1+x^2}, \qquad \sin^2\theta = \frac{x^2}{1+x^2}, \tag{D66}$$

gives

$$\frac{\Lambda_\delta}{\delta}\sum_\ell p_\ell\left(U_{\ell,\delta}(\cdot)U^\dagger_{\ell,\delta} - \mathrm{id}\right) = -i\frac{\Lambda_\delta}{\delta}\frac{x}{1+x^2}\sum_\ell p_\ell s_\ell[P_\ell,\cdot] \tag{D67}$$

$$+\frac{\Lambda_\delta}{\delta}\frac{x^2}{1+x^2}\sum_\ell p_\ell\mathcal{Z}_{P_\ell}. \tag{D68}$$

Because

$$\Lambda_\delta = \Gamma(1+x^2), \qquad x = \frac{\delta\lambda}{\Gamma}, \qquad p_\ell s_\ell = \frac{h_\ell}{\lambda}, \tag{D69}$$

the first term is

$$-i\sum_\ell h_\ell[P_\ell,\cdot] = \mathcal{L}_H. \tag{D70}$$

The second term is

$$\frac{\Gamma(1+x^2)}{\delta}\frac{x^2}{1+x^2}\sum_\ell p_\ell\mathcal{Z}_{P_\ell} = \frac{\delta\lambda^2}{\Gamma}\sum_\ell p_\ell\mathcal{Z}_{P_\ell} = \frac{\delta\lambda}{\Gamma}\sum_\ell|h_\ell|\mathcal{Z}_{P_\ell}. \tag{D71}$$

This proves the claim. □

The usual qDRIFT step angle is $\lambda t/N$, where N is the number of random Pauli rotations. In the Poissonized process above, if $N = \mathbb{E}N_T$, then

$$\frac{\lambda t}{N} = \sin\theta\cos\theta. \tag{D72}$$

For small δ, $\sin\theta\cos\theta = \theta + O(\theta^3)$, so the kick angle itself agrees with the qDRIFT angle to leading order. The exact matching is at the generator level, through the coefficient $\sin\theta\cos\theta$.

Corollary 1 (Autonomous qDRIFT scaling)**.** *Choose the optimal rates $\gamma_\ell^\star$. Then*

$$e^{(s/\delta)\mathcal{L}^{(+)}_{\delta,\gamma^\star}}$$

simulates $e^{s\mathcal{L}_H}$ uniformly for $0 \le s \le t$ with error at most ϵ whenever

$$0 < \delta \le \frac{\epsilon\Gamma}{2t\lambda^2}. \tag{D73}$$

Equivalently, the required dissipative time is

$$T = \frac{t}{\delta} = O\left(\frac{t^2\lambda^2}{\Gamma\epsilon}\right). \tag{D74}$$

If δ saturates eq. (D73), then the expected number of jumps up to final time T is

$$\mathbb{E}N_T = \Lambda_\delta T = \frac{2t^2\lambda^2}{\epsilon} + \frac{\epsilon}{2}. \tag{D75}$$

Proof. By eq. (D62),

$$\frac{1}{\delta}\mathcal{L}^{(+)}_{\delta,\gamma^\star} = \mathcal{L}_H + \frac{\delta\lambda}{\Gamma}\sum_\ell |h_\ell|\mathcal{Z}_{P_\ell}. \tag{D76}$$

The diffusion term has diamond norm at most

$$\frac{\delta\lambda}{\Gamma}\sum_\ell |h_\ell|\|\mathcal{Z}_{P_\ell}\|_\diamond \le \frac{2\delta\lambda^2}{\Gamma}. \tag{D77}$$

Duhamel's identity therefore gives error at most $2t\delta\lambda^2/\Gamma$, proving eq. (D73) and eq. (D74).

For the expected number of jumps, use

$$\Lambda_\delta = \Gamma(1+x^2), \qquad x = \frac{\delta\lambda}{\Gamma}. \tag{D78}$$

Thus

$$\mathbb{E}N_T = \Lambda_\delta\frac{t}{\delta} = \frac{\Gamma t}{\delta} + \frac{\delta\lambda^2 t}{\Gamma}. \tag{D79}$$

Substituting

$$\delta = \frac{\epsilon\Gamma}{2t\lambda^2} \tag{D80}$$

gives

$$\mathbb{E}N_T = \frac{2t^2\lambda^2}{\epsilon} + \frac{\epsilon}{2}. \tag{D81}$$

□

In essence, we see that the bath realizes an autonomous, Poissonized qDRIFT channel: the jump label distribution is exactly $|h_\ell|/\lambda$, the kick angle is term-independent, and the expected number of kicks has the standard $O(t^2\lambda^2/\epsilon)$ scaling.

Appendix E: Dissipative FLO for observable estimation

The construction of Hamiltonian dynamics from dissipation also gives a post-processed simulation primitive in the spirit of qFLO [33]. The key point is that, after rescaling time, the artificial dissipative error is a controlled step-size error. By varying this step size and extrapolating expectation values to the zero-step-size limit, one can improve the dependence on the target precision for observable estimation even exponentially.

We first describe the clean linear-flow setting. Let

$$\Phi_s(t) := e^{(t/s)\mathcal{L}_{D,s}} = e^{t(\mathcal{L}_H + s\mathcal{R})}, \qquad 0 < s < s_0, \tag{E1}$$

where

$$\mathcal{L}_H(\rho) = -i[H, \rho], \tag{E2}$$

and $\mathcal{R}$ is a bounded Lindbladian. For the single-jump construction $F_s = I - isH$, one has

$$\mathcal{R} = \mathcal{D}_H, \qquad \mathcal{D}_H[\rho] = H\rho H - \frac{1}{2}\{H^2, \rho\}. \tag{E3}$$

For a decomposition $H = \sum_\ell H_\ell$ with jumps $F_{\ell,s} = I - isH_\ell$, one has

$$\mathcal{R} = \sum_\ell \mathcal{D}_{H_\ell}. \tag{E4}$$

Thus the parameter s plays the role of an inverse depth or step size: smaller s gives a more accurate physical dissipative channel, but requires a longer dissipative evolution time t/s.

Let O be an observable and define

$$f_O(s, t; \rho) := \mathrm{Tr}[O\, \Phi_s(t)(\rho)]\,. \tag{E5}$$

The ideal Hamiltonian value is

$$f_O(0, t; \rho) = \mathrm{Tr}\big[O\, e^{t\mathcal{L}_H}(\rho)\big]\,. \tag{E6}$$

Since $\Phi_s(t) = e^{t(\mathcal{L}_H + s\mathcal{R})}$ is analytic in s, we may expand

$$f_O(s, t; \rho) = f_O(0, t; \rho) + \sum_{r \geq 1} a_r(t, \rho, O) s^r. \tag{E7}$$

A Richardson extrapolator cancels the first several powers of s.

We use the same well-conditioned choice of Richardson nodes as in well-conditioned multiproduct formulas and qFLO. For an integer $m \geq 2$, set

$$R_m := \sqrt{\frac{8m}{\pi}}, \qquad x_j^{(2m)} := \sin^2\!\left(\frac{\pi(2j-1)}{8m}\right), \qquad y_j := \left\lceil \frac{R_m}{\sqrt{x_j^{(2m)}}} \right\rceil^2, \tag{E8}$$

for $j = 1, \ldots, m$. Given a largest step size s_m, define

$$s_j := s_m \frac{y_m}{y_j}, \qquad j = 1, \ldots, m. \tag{E9}$$

The Richardson weights are

$$b_j := \prod_{\ell \neq j} \frac{1}{1 - y_\ell / y_j}. \tag{E10}$$

They satisfy

$$\sum_{j=1}^m b_j = 1, \qquad \sum_{j=1}^m b_j s_j^r = 0, \qquad r = 1, \ldots, m-1. \tag{E11}$$

Moreover, this choice is well-conditioned:

$$\|b\|_1 := \sum_{j=1}^{m} |b_j| = O(\log m), \qquad \max_j \frac{y_j}{y_m} = O(m^2). \tag{E12}$$

Define the m-point dissipative-FLO estimator

$$\widehat{f}_m(s_m, t; \rho, O) := \sum_{j=1}^{m} b_j f_O(s_j, t; \rho). \tag{E13}$$

We then have:

Theorem 5 (qFLO-style dissipative extrapolation)**.** *Let $\Phi_s(t) = e^{t(\mathcal{L}_H + s\mathcal{R})}$, and define $B := \|\mathcal{R}\|_\diamond$. Suppose $\|O\|_\infty \leq 1$. Then the Richardson estimator in eq. (E13) satisfies*

$$\left|\widehat{f}_m(s_m, t; \rho, O) - \mathrm{Tr}\big[O\, e^{t\mathcal{L}_H}(\rho)\big]\right| \leq 2\|b\|_1 \left(\frac{e\, tB\, s_m}{m}\right)^m \tag{E14}$$

whenever $tBs_m \leq m/2$. Consequently, choosing

$$\frac{1}{s_m} = \Theta\left(\frac{tB}{m}\left(\frac{\|b\|_1}{\epsilon}\right)^{1/m}\right) \tag{E15}$$

gives intrinsic extrapolation error at most ϵ. With the well-conditioned nodes above, the maximum inverse step size is

$$N_{\max} := \max_j \frac{1}{s_j} = O\left(tB\, m\left(\frac{\log m}{\epsilon}\right)^{1/m}\right). \tag{E16}$$

Taking $m = \Theta(\log(1/\epsilon))$ yields

$$N_{\max} = O(tB \log(1/\epsilon))\,, \tag{E17}$$

and hence the largest dissipative evolution time among the extrapolation runs is

$$T_{\max} := \max_j \frac{t}{s_j} = O\big(t^2 B \log(1/\epsilon)\big)\,. \tag{E18}$$

Proof. By iterating Duhamel's identity, for $s \geq 0$ we have

$$e^{t(\mathcal{L}_H + s\mathcal{R})} = e^{t\mathcal{L}_H} + \sum_{r=1}^{m-1} s^r \int_{0 \leq u_r \leq \cdots \leq u_1 \leq t} e^{(t-u_1)\mathcal{L}_H} \mathcal{R} e^{(u_1-u_2)\mathcal{L}_H} \cdots \mathcal{R} e^{u_r \mathcal{L}_H}\, du_1 \cdots du_r + \mathcal{E}_m(s,t), \tag{E19}$$

where the remainder satisfies

$$\|\mathcal{E}_m(s,t)\|_\diamond \leq \sum_{r=m}^{\infty} \frac{(tBs)^r}{r!}. \tag{E20}$$

Here we used that all semigroups in the integrand are completely positive and trace preserving and hence have diamond norm at most one.

Taking expectation values against O gives a power series in s. The conditions $\sum_j b_j s_j^r = 0$ for $r = 1, \ldots, m-1$ cancel the first $m-1$ terms. Therefore

$$\left|\widehat{f}_m(s_m, t; \rho, O) - f_O(0, t; \rho)\right| \leq \sum_{j=1}^{m} |b_j| \|O\|_\infty \|\mathcal{E}_m(s_j, t)\|_\diamond \tag{E21}$$

$$\leq \|b\|_1 \sum_{r=m}^{\infty} \frac{(tBs_m)^r}{r!}, \tag{E22}$$

because $s_j \le s_m$. If $tBs_m \le m/2$, then

$$\sum_{r=m}^{\infty} \frac{(tBs_m)^r}{r!} \le 2\frac{(tBs_m)^m}{m!} \le 2\left(\frac{e\,tB\,s_m}{m}\right)^m, \tag{E23}$$

where the last inequality uses $m! \ge (m/e)^m$. This proves eq. (E14). Solving the right-hand side for s_m gives eq. (E15). Finally,

$$N_{\max} = \max_j \frac{1}{s_j} = \frac{1}{s_m}\max_j \frac{y_j}{y_m} = O\left(m^2 \frac{1}{s_m}\right). \tag{E24}$$

Using $\|b\|_1 = O(\log m)$ gives eq. (E16). Taking $m = \Theta(\log(1/\epsilon))$ gives $(\log m/\epsilon)^{1/m} = O(1)$, and hence eq. (E17) and eq. (E18). □

Several comments are important. First, $\widehat{f}_m$ is a classical post-processed estimator, not the expectation value of a physical CPTP channel: some Richardson weights are negative. Thus theorem 5 does not contradict the physical lower bound in theorem 2. The lower bound concerns a genuine dissipative channel approximating the Hamiltonian channel in diamond norm, whereas theorem 5 concerns observable estimation via a signed combination of data from several physical dissipative experiments.

Second, the estimator is robust to measurement error. Suppose each value $f_O(s_j, t; \rho)$ is estimated up to additive error ϵ_{data}. Then the induced error in $\widehat{f}_m$ is at most

$$\|b\|_1 \epsilon_{\text{data}}. \tag{E25}$$

Thus it suffices to estimate each data point to precision

$$\epsilon_{\text{data}} = O\left(\frac{\epsilon}{\|b\|_1}\right). \tag{E26}$$

Since $\|b\|_1 = O(\log m) = O(\log\log(1/\epsilon))$ for $m = \Theta(\log(1/\epsilon))$, the shot overhead remains essentially the usual observable-estimation overhead. For bounded observables, Hoeffding's inequality gives

$$N_{\text{shots}} = \widetilde{O}(1/\epsilon^2) \tag{E27}$$

shots per extrapolation point.

For the single-jump construction, $B = \|\mathcal{D}_H\|_\diamond \le 2\|H\|_\infty^2$. Therefore, dissipative FLO estimates observables with intrinsic bias ϵ using largest dissipative evolution time

$$T_{\max} = O\left(t^2\|H\|_\infty^2 \log(1/\epsilon)\right), \tag{E28}$$

rather than the physical-channel scaling

$$O\left(t^2\|H\|_\infty^2/\epsilon\right). \tag{E29}$$

For the autonomous qDRIFT construction of App. D, one has

$$\mathcal{R}_\gamma = \sum_\ell \frac{h_\ell^2}{\gamma_\ell}\mathcal{Z}_{P_\ell}, \qquad \|\mathcal{R}_\gamma\|_\diamond \le 2S_\gamma, \qquad S_\gamma = \sum_\ell \frac{h_\ell^2}{\gamma_\ell}. \tag{E30}$$

With the optimal rate allocation

$$\gamma_\ell^\star = \Gamma\frac{|h_\ell|}{\lambda}, \qquad \lambda = \sum_\ell |h_\ell|, \tag{E31}$$

we have

$$S_{\gamma^\star} = \frac{\lambda^2}{\Gamma}. \tag{E32}$$

Hence the dissipative-FLO version of autonomous qDRIFT has largest dissipative time

$$T_{\max} = O\left(\frac{t^2\lambda^2}{\Gamma}\log(1/\epsilon)\right), \tag{E33}$$

and the corresponding expected number of Poisson kicks scales as

$$\mathbb{E}N_{\max} = O\big(t^2\lambda^2 \log(1/\epsilon)\big)\,, \tag{E34}$$

up to constants and logarithmic factors from the conditioning of the Richardson estimator. This is the direct dissipative analogue of the qFLO improvement from qDRIFT's $1/\epsilon$ depth dependence to logarithmic dependence in $1/\epsilon$, for observable estimation rather than state preparation.